

Ultra-Efficient Small Turbine Engines

Nathan Genrich,¹ Crawford Leeds,² and Tyler Smith³
University of Colorado, Boulder, CO, 80503

This paper serves to provide an analysis on small, thrust producing, gas turbine engines to provide a foundation to future development on engine efficiency. Small gas turbines have been employed on a relatively small market of government unmanned aircraft and hobbyists with loose fuel consumption requirements. In the past decade large gas turbine engines for private and commercial aircraft have decreased thrust specific fuel consumption by approximately 20%. A significant driver of this is the increased cost of fuel and consumers' demand for low airfare. Until recently the small turbine market has been too small to demand high fuel efficiency. Advances to the autonomous and unmanned aircraft industry has increased demand for relatively small aircraft. Operators are now managing a much larger fleet and therefore can find large cost savings from increasing fuel efficiency. Extended unmanned aircraft operations has also become increasingly valuable for military reconnaissance. Now that there is potential for large cost savings with increasing fuel efficiency, the United States Air Force is pursuing a competition for an ultra-efficient jet engine for unmanned aircraft applications. The conclusion of this paper will describe the shortfalls of current small aircraft and the critical components that can contribute to meeting the competitions strict requirements.

Nomenclature

a	=	Speed of sound
CFD	=	Computational Fluid Dynamics
C_{pc}	=	Compressor specific heat at constant pressure
C_{pt}	=	Turbine specific heat at constant pressure
f	=	Fuel-to-air ratio
h_{pr}	=	Fuel heating value
M	=	Mach number
P	=	Pressure
P_t	=	Stagnation pressure
R_c	=	Compressor gas constant of air
R_t	=	Turbine gas constant of air
S_T	=	Specific thrust
S_{fc}	=	Thrust specific fuel consumption
T	=	Temperature
T_t	=	Stagnation temperature
u	=	Flow velocity
η	=	Efficiency
γ_c	=	Ratio of specific heats in compressor
γ_t	=	Ratio of specific heats in turbine
π	=	Pressure ratio
τ	=	Temperature ratio

¹ BS/MS Student, Aerospace Engineering Sciences

² BS/MS Student, Aerospace Engineering Sciences

³ BS/MS Student, Aerospace Engineering Sciences

I. Introduction

SMALL gas turbine engines are a field that has high growth potential but has not been fully explored yet. However, the Air Force has recently put out a challenge to develop a small, high efficiency turboprop or turboshaft engine for small unmanned aerial vehicles. The recent enormous increase in the drone market due to military demand makes such an endeavor potentially very profitable. Currently, the majority of the unmanned aerial systems employed by the US military are powered by internal combustion engines. Examples of this include the General Atomics Predator and Reaper. Although there are gas turbine engine-powered unmanned vehicles, it is a largely unexplored market because of the inefficiencies and poor performance associated with small-scale gas turbine engines.

There are a number of problems associated with small gas turbine engines which make them perform worse in terms of both efficiency and total thrust/power. Beyond the fact that there has only been recent demand for high-performance micro engines, technical problems such as cooling, manufacturing of small parts, limited configurations for rotating parts, and many other issues have to be dealt with.

With this in perspective, the goal of this project was to determine how to alter parameters of a set of already-existing small-scale gas turbine engines in order to meet performance requirements set out by the Air Force challenge. On top of this, technologies were researched that could potentially make such an improvement in performance possible.

II. Problem Definition

The Air Force challenge outlines several requirements for small engines. Several pertinent requirements have been compiled in Table 1 below:

Table 1: Air Force challenge parameters

Variable	Value
Fuel type	Jet A fuel
Power output	50 bhp – 150 bhp max continuous output
BSFC	0.55 lbm/bhp-hr
Specific power	2.0 bhp/lb
Maximum weight	75 lb

Note that these values, especially the BSFC and specific power, seem like extremely easily achievable goals for an engine. [1] provides a set of military turboprop and turboshaft engines and their known specifications. The team performed some calculations on this data set and found that the average specific power on this data set was 2.49 bhp/lb and the average BSFC was 0.562 lbm/bhp-hr. Both of these values barely exceed the requirements set out by the challenge. If an average performing turboprop engine can already exceed the specifications, it stands to reason that such a thing would be possible for small engines. Again, however, these specifications are difficult to meet due to technical problems and low technology readiness levels for such small machines.

The team did not focus on turboprop engines; rather, due to an interest in turbojets, these were used instead. Unfortunately, the metrics by which turboprops are measured are not the same metrics by which turbojets and turbofans are measured. In order to provide new metrics, a different scheme had to be decided upon. Notice how the average of the large-scale turboprop engines very nearly met the requirements for the small-scale engines. Because of this consideration, the team used a set from [1] describing large-scale military turbofan and turbojet engines. Over 1000 engines were analyzed from the database. Performing similar analysis on this data set, it was found that the average specific thrust for these engines was 1800 ft/s and the average TSFC was 0.873 (in English units). These averages for the large scale engines were used as a modified set of requirements for the new small-scale engine. The new requirements have been compiled in Table 2:

Table 1: Modified challenge parameters

Variable	Value
Fuel type	Any
TSFC	0.873 lb _f /lb _m -hr
Specific thrust	1800 ft/s
Maximum weight	75 lb

At this point, the problem was fully defined. The next step was to pick engines for analysis, determine their baseline values, and try to optimize parameters to meet the goals of the project. Analysis will be presented in the next section, but the engines chosen were the Jet Cat P90-RXI, and the Jet Cat P200-SE. These were chosen because of the team's previous experience with these two engines as well as the fact that several important values for analysis have been explored by the team previously. This was very desirable due to the fact that less assumptions had to be made about values such as efficiency, pressure ratios, and many other values.

III. Analysis

A. Methodology for Real Cycle Analysis

Before doing any analysis specific to an engine, a function was created to perform cycle analysis of an engine assuming imperfect and irreversible processes. A real cycle analysis differs greatly from an ideal cycle analysis and includes more real life considerations to give a better model of engine performance. Real cycle analysis accounts for changing gas properties as the flow traverses through the engine. More specifically, the temperature changes greatly across the compressor, turbine, and combustor, and therefore changes the specific heat. The real cycle analysis also accounts for losses in the inlet, compressor, and turbine. Additionally, incomplete combustion and stagnation pressure losses in the combustor are considered. Finally, non-isentropic expansion in the nozzle is taken into account. These combined considerations result in a more realistic, and therefore more accurate model of the engine.

Real cycle analysis does not work without inputs. For purposes of this project, several variables were assumed to be constant regardless of the engine being considered:

$$\gamma_c = 1.4, \quad \gamma_t = 1.33, \quad R_c = R_t = 287 \frac{J}{kgK}, \quad c_{pc} = 1004 \frac{J}{kgK}, \quad c_{pt} = 1156 \frac{J}{kgK}, \quad M_\infty = 0$$

In addition to these values, there were several inputs specific to each engine, including the efficiencies for all engine stages, turbine entry temperature, compressor pressure ratio, and fuel heating value. With this in mind, analysis could begin:

First, need to calculate the recovery ratios for pressure and temperature using the freestream conditions. The ultimate goal was to get pressure and temperature ratios for all of the different engine stations, and then be able to calculate exit properties and thrust.

$$\tau_r = 1 + \frac{\gamma_c - 1}{2} M_\infty^2$$

$$\pi_r = \tau_r^{\frac{\gamma}{\gamma-1}}$$

The next value that could be calculated was the

$$\tau_\lambda = \frac{c_{pt} T_{t4}}{c_{pc} T_0}$$

With all of the previous values, the fuel to air ratio could be calculated:

$$f = \frac{\tau_\lambda - \tau_r \tau_c}{\frac{\eta_b h_{pr}}{c_{pc} T_0} - \tau_\lambda}$$

At this point, turbine pressure and temperature ratios could be calculated:

$$\tau_t = 1 - \frac{\tau_r \tau_c}{\tau_\lambda \eta_m (1 + f)}$$

$$\pi_t = \frac{\tau_t^{\gamma_t}}{e_t (\gamma_t - 1)}$$

Once all of the pressure and temperature ratios for each stage were calculated, the exit properties were calculated starting with the stagnation pressure ratio

$$\frac{p_{t9}}{p_9} = \pi_r \pi_d \pi_c \pi_b \pi_t \pi_n \frac{p_0}{p_9}$$

Using the stagnation pressure ratio, the exit Mach number was calculated:

$$M_9 = \left(\frac{2}{\gamma_t - 1} \right) \left(\frac{p_{t9}}{p_9} \right)^{\frac{\sqrt{\gamma_t - 1}}{\gamma_t}}$$

After this, the exit temperature ratio was calculated:

$$\frac{T_9}{T_0} = \frac{\frac{c_{pc}}{c_{pt}} \tau_\lambda \tau_t}{\left(\frac{p_{t9}}{p_9}\right)^{\frac{\gamma_t-1}{\gamma_t}}}$$

The purpose of this exit temperature ratio was to calculate the speed of flow at the exit:

$$\frac{u_9}{a_0} = M_9 \sqrt{\frac{T_9 \gamma_t}{T_0 \gamma_c}}$$

Finally, the ultimate goal of the project could be calculated: the specific thrust.

$$S_T = a_0 \left((1+f) \frac{u_9}{a_0} - M_\infty + \frac{1+f}{\gamma} \frac{T_9}{T_0} \frac{a_0}{u_9} \left(1 - \frac{p_0}{p_9}\right) \right)$$

This allowed for calculation of the thrust specific fuel consumption.

$$S_{fc} = \frac{f}{S_T}$$

All of the necessary values have been calculated by this point. Out of curiosity, the thermal, propulsive, and overall efficiencies were also calculated:

$$\eta_{th} = a_0^2 \frac{\left((1+f) \left(\frac{u_9}{a_0}\right)^2 - M_\infty^2 \right)}{2f h_{pr}}$$

$$\eta_p = 2S_T \frac{M_0}{a_0 \left((1+f) \left(\frac{u_9}{a_0}\right)^2 - M_0^2 \right)}$$

$$\eta_0 = \eta_{th} \eta_p$$

This was a brief outline of the methodology used for full turbojet cycle analysis. For insight to the implementation of this method, see Appendix A for Matlab code.

B. Baseline Performance for Chosen Engines

Table 1: JetCat Engine Characteristics

Engine	Compressor Pressure Ratio	Turbine Entry Temperature (K)	Compressor Efficiency	Turbine Efficiency
JetCat P90RXI	2.6	1325	47%	90%
JetCat P200	4.0	1325	44%	90%

From the above table, the compressor pressure ratio, turbine entry temperature and compressor efficiencies were determined from documentation on the JetCat engines. The turbine efficiency was not given in documentation, so they were determined using the polytropic efficiencies, assuming a polytropic efficiency of 0.9, which is a typical value for jet engines. Using these, a real cycle analysis was performed, the results of which are shown in the following table

Table 2: JetCat Engine Performance Characteristics

Engine	ST (ft/s)	TSFC (lb/lb _m /hr)
JetCat P90RXI	1531	1.87
JetCat P200	1462	1.72

The P90RXI, which is a smaller engine, has a slightly larger specific thrust; however, it also has a much higher thrust specific fuel consumption. Both engines fail to meet the criteria for the turbine prize which states that the

specific thrust must be at least 1800 ft/s and TSFC must be less than 0.87. This lead to a performance analysis in order to determine what characteristics of the engines could be altered in order to meet the criteria for the prize. The efficiencies used in the analysis are as follows. These are general values not specific to the JetCat engines; however, these parameters could be easily altered if a specific study on the JetCat engines was desired.

$$\begin{aligned} \eta_m &= 0.99 \\ \eta_b &= 0.99 \\ \eta_t &= 0.92 \\ \eta_c &= 0.92 \end{aligned}$$

It is important to note that the static conditions were analyzed; therefore, the flight speed was set to 0 and the temperature used was that at sea level conditions. The results were compared against the requirements of the turbine prize. More specifically, the specific thrust had to be at least 1800 ft/s and the thrust specific fuel consumption had to be less than 0.87 lbf/lbm/hr.

C. Parameter Optimization

Using the real cycle analysis, a parameter study was performed to determine the performance of different engines with different characteristics. An investigation of the effect of turbine entry temperature and compressor pressure ratio was performed by varying the parameters in the real cycle analysis. The turbine entry temperature was varied from 1300 K to 2400 K, a range which includes that for both small engines and large commercial engines. The high end of the range, 2400 K, is the adiabatic flame temperature of JetA, which is the highest TET achievable, and the low end of the range, 1300K, is characteristic of smaller engines that use different materials and don't have adequate cooling systems to support a higher turbine entry temperature. The compressor pressure ratio was varied from 2 to 35 which includes smaller engines that have lower pressure ratios and commercial jet engines which have pressure ratios up to as much as 35 (GE F100, GE F118). As a baseline, the JetCat P90RXI and JetCat P200 were analyzed. A performance analysis was then performed by varying the turbine entry temperature and the compressor pressure ratio around the values for the two JetCat engines.

The results of the general parameter study are shown below. A plot of the specific thrust is shown following

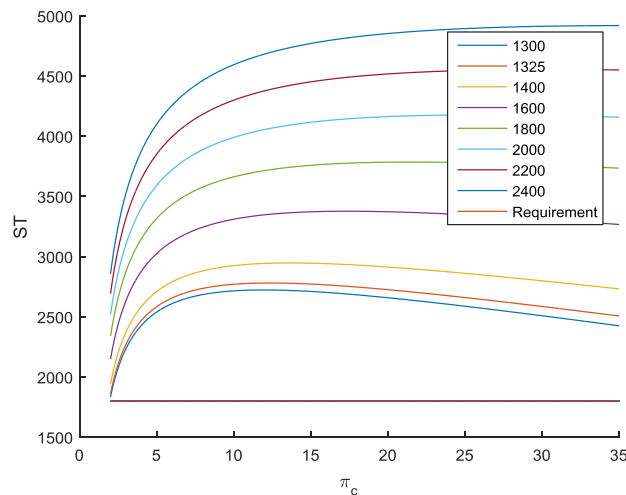


Figure 1: Specific Thrust

The plot shows the relationship between the specific thrust and the compressor pressure ratio, with each curve representing a different value for the turbine entry temperature, as defined in the legend. The plot also has the requirement for the Air Force turbine prize of a specific thrust greater than or equal to 1800 ft/s. As the results demonstrate, the specific thrust requirement is met for each value of turbine entry temperature for every compressor pressure ratio. Additionally, the results demonstrate that the specific thrust increases with turbine entry temperature.

The next parameter analyzed was the thrust specific fuel consumption. The results can be seen in the following figure

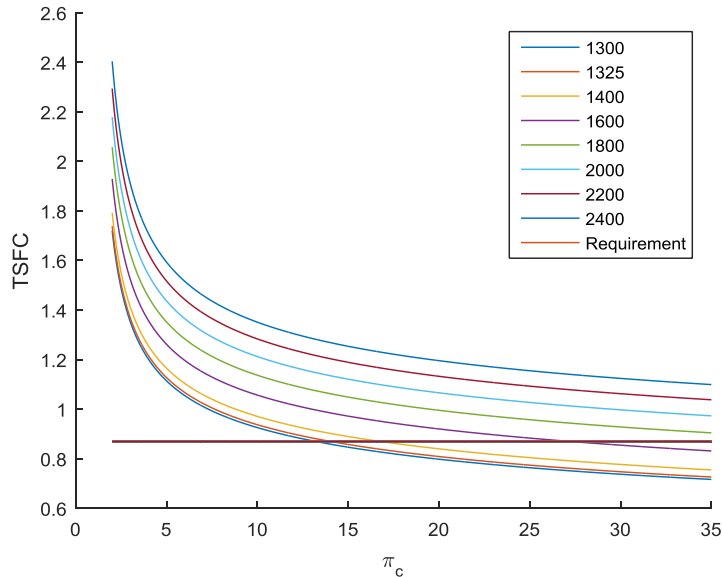


Figure 2: Thrust Specific Fuel Consumption

The results of the analysis show that the thrust specific fuel consumption requirement is very constraining. The thrust specific fuel consumption was plotted as a function of compressor pressure ratio, with the various curves representing different values of turbine entry temperature. The figure also shows the requirement for the turbine prize of a TSFC less than 0.873 lb_f/lb_m/hr. As the plot demonstrates, to meet the requirement the compressor pressure ratio must be at least 15 for low values of turbine entry temperature. However, for larger turbine entry temperatures, the compressor pressure ratio needed to meet the requirement greatly increases. This demonstrates the challenging nature of the turbine prize. In order to meet the TSFC requirement, the pressure ratio must be greater than 15. This is less challenging for large commercial jet engines; however, since this prize is geared towards small turbine engines, this requirement becomes much more constraining. To give insight into how constraining this is, the compressor pressure ratio for the JetCat P90RXI is 2.6 and the pressure ratio for the JetCat P200-SE is 4.0. Although these engines are on the smaller end – 3.16 lb. and 5.23 lb. respectively – they would require more stages to meet the requirement. Increasing the number of stages would increase the size and mass. These engines have over 60 pounds of margin to meet the competition requirements, but continuous growth in the number of stages and compressor size will eventually cause the mass constraint to become a serious concern.

Even with an axial compressor, the compressor pressure ratio can be achieved through the use of multiple stages. This demonstrates that the turbine prize is feasible; however, more advanced techniques would be required to meet the performance requirements while simultaneously meeting the size requirements.

To analyze the ideal case, the component efficiencies were all set to unity and the performance characteristics were analyzed. The results for the thrust specific fuel consumption are shown in the following figure.

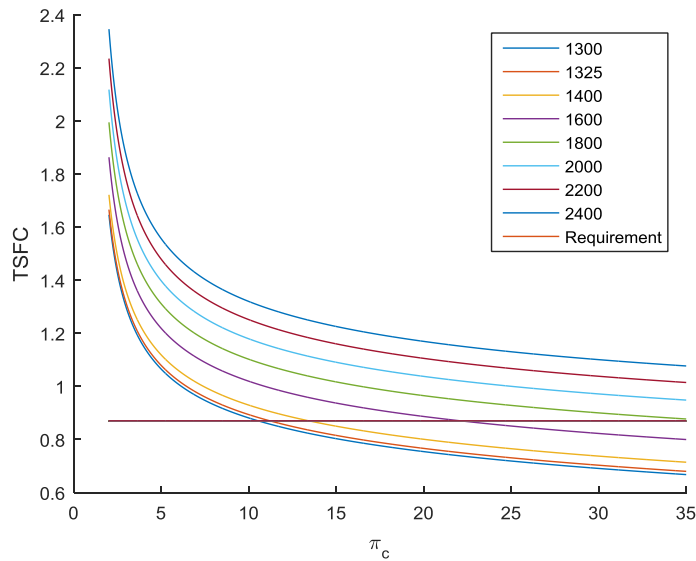


Figure 3: Thrust Specific Fuel Consumption-Ideal Case

The figure shows that the compressor pressure ratio needed to meet the requirement for the turbine prize is much less than that for component efficiencies less than unity. Therefore, if work is done to improve the component efficiencies, the pressure ratio requirement could be met with fewer stages, therefore reducing size and weight.

D. Methods and Feasibility of Reaching Optimized Parameters

Almost all small commercially available jet turbine engines – including the JetCat P90-RXi and JetCat P200-SE – use centrifugal compressors. This is due to their compact size, ease of manufacturing, and high pressure ratio per stage. The analysis from the previous section showed that the JetCat engines could meet the competition requirements by creating a very high pressure ratio – on the order of $\pi_c = 15$. Now that the true manufacturing goal for a small engine has been defined, the true challenge is in designing components to support this requirement. This asks for a compressor pressure ratio increase of 600%. There are many technologies that could support this, all of which could add manufacturing complexity, increased thermal loads, and potential for price increases.

Large modern engines use almost exclusively axial compressors rather than centrifugal compressors. This requires multiple stages as the pressure ratio across each stage is less than it is for a centrifugal compressor. However, engines such as the Pratt and Whitney F100 has an overall pressure ratio of 35 and the GE F118 has an overall pressure ratio of 35.1. This proves that it is possible to have an axial compressor than can support pressure ratios above 15 as needed for this competition. It may be possible to have a multi stage compressor achieve the same compressor pressure ratio, but this is generally not considered practical due to the extremely large intake required and the efficiencies lost due to redirecting flow. Thus, a multi-stage axial compressor will be considered the most viable option for achieving a minimum overall pressure ratio of 15.

One of the first considerations in increasing the pressure is the increased temperatures found in the combustor, and therefore the turbines. The turbine blades are made of Inconel – an alloy of nickel containing chromium and iron. Inconel has a melting temperature of 1673 K. Currently the JetCat engines have a burner temperature around 1350 K. The maximum increase in temperature would be from assuming an isentropic relationship. Thus, the temperature increase corresponding to a pressure ratio of 2.6 and 15 can found using the following method.

$$\frac{T_2}{T_1} = \pi_c^{\frac{\gamma-1}{\gamma}}$$

For the JetCat P90-RXi,

$$\frac{T_2}{T_1} = 2.6^{\frac{.4}{1.4}} = 1.39$$

For the JetCat P200-SE

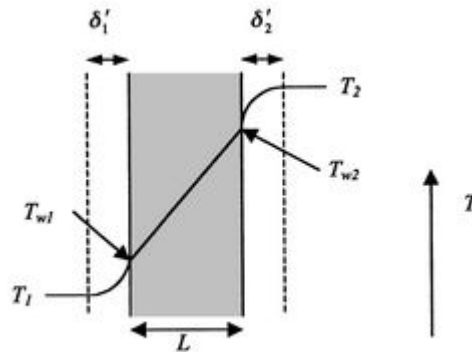
$$\frac{T_2}{T_1} = 4^{\frac{.4}{1.4}} = 1.48$$

Now, for an engine with a compressor pressure ratio of 15,

$$\frac{T_2}{T_1} = 15^{\frac{.4}{1.4}} = 2.17$$

Thus, increasing the pressure ratio to 15 or more will increase the temperature increase across the compressor by a minimum of 50%. It may be required that another component of the engine is changed to prevent the turbine blades from deforming to the point of seizing the motor. One of common methods of accomplishing this is by cooling the turbine blades. An analysis was done on a motor that has a combustor temperature of 2200 K, uses Inconel turbine blades, and has cool air rushing inside the turbine blades to remove heat. This analysis is outlined below.

The analysis was performed by using combined conduction and convection equations. The figure below shows a cutaway of a turbine blade.



In the figure above, L is the thickness of the blade. T_1 is the temperature of cool air inside the blade, T_{w1} is the temperature of the inside wall of the blade, T_{w2} is the wall temperature of the outside of the blade (hottest point on the blade), and T_2 is the temperature of the hot air around the blades. δ_1 and δ_2 represent the size of the thermal boundary layer. The equations for the heat transfer per unit area is shown below.

Convection inside the blade:

$$\frac{\dot{Q}}{A} = h_1(T_{w1} - T_1)$$

Conduction through the blade:

$$\frac{\dot{Q}}{A} = \frac{k}{L}(T_{w2} - T_{w1})$$

Convection through the outer thermal boundary layer of the blade:

$$\frac{\dot{Q}}{A} = 2(T_2 - T_{w2})$$

Setting each $\frac{\dot{Q}}{A}$ equal and recognizing $\dot{Q} = \frac{T_2 - T_1}{R}$ where R is the thermal resistance $R = \frac{1}{h_1 A} + \frac{L}{Ak} + \frac{1}{h_2 A}$ we can solve directly for T_{w2} .

$$T_{w2} = T_2 - \frac{T_2 - T_1}{\frac{h_2}{h_1} + \frac{Lh_2}{k} + 1}$$

This shows a linear relationship between the internal air temperature and the maximum blade temperature. It was assumed that there was air within the blade, and air (no burned fuel) outside the blade. The blade thickness was assumed to be 2 mm. The following coefficients were also defined.

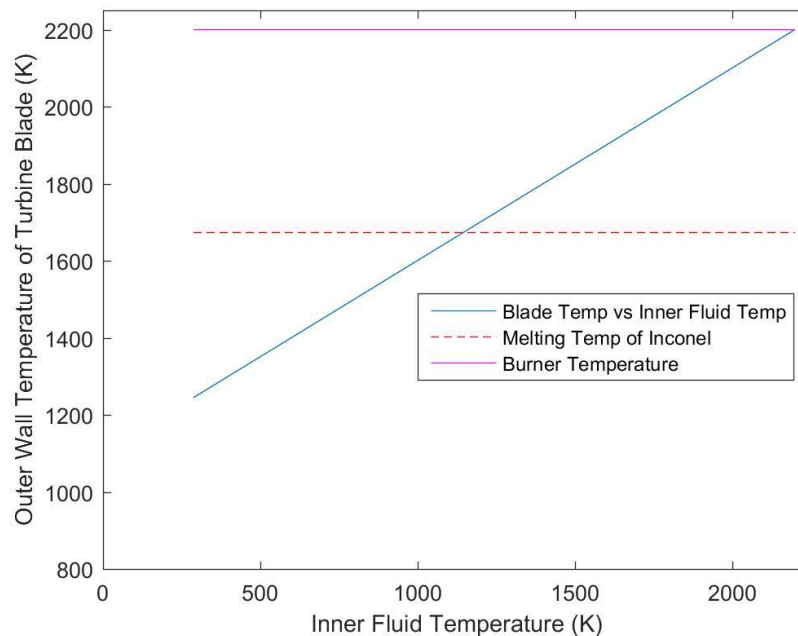
Thermal conductivity,

$$k = 6.5 \frac{W}{m K}$$

Coefficient of thermal convection,

$$h_1 = h_2 = 7 \frac{W}{m^2 K}$$

Below is a table of the maximum blade temperature vs. the temperature of the air inside the blade.



It is obvious that as the inner air temperature reaches the combustor temperature, there is effectively no cooling as the maximum blade temperature reaches the combustor temperature. At a combustor temperature of 2200 K it shows that the air inside the blade must stay at 1100 K or cooler to keep the turbine from melting. It should stay at around 600 K to maintain the JetCat blades at the same temperature the turbine blades are at before any modification. In order to do this air must be circulated outside (or through a refrigeration unit) and the inside of the turbine blades.

This analysis does make some linearizing assumptions, but it shows an approximate requirement on the system to maintain the turbine blades at a safe temperature with a combustor temperature at values that approach the adiabatic flame temperature. This research did not attempt to quantify the complexity or specific manufacturing means of applying cooling air inside the turbine blades. Rather, qualitatively it must be understood that there poses a serious challenge to apply cooling air inside the blades while maintaining the appropriate size and thickness of each blade to maintain its desired aerodynamic properties.

By adding an effectively larger compressor, the single turbine stage in both JetCat engines may not be enough. It is definite that more power will need to be extracted from the turbine to drive the larger compressor. This could be

accomplished in multiple ways – all would increase the price of the engine and add complexity. These engines were designed many years ago before some of the recent advancements in computational fluid dynamics. A new computational fluid dynamics model could be used to obtain a more efficient turbine. Additional stages could be added to extract more power. Some combination of additional stages and an advanced CFD model could also be applied.

The increased pressure ratio in the compressor does not only create a higher turbine entry temperature, but it adds strain to the compressor components, and especially the combustor. Most combustors are constant pressure combustors, which means that the combustor entry temperature must be held throughout the combustion process. The combustors used in the JetCat engines are can-type combustors. Thus, increasing the pressure ratio would increase the hoop stress. By increasing the pressure ratio from 4 to 16 would increase the hoop stress by a factor of 4. To keep the same hoop stress and the same combustor material, the thickness would have to increase by a factor of 4. This is a significant change and would add significantly to the mass of the engine. The current thickness of the steel combustion chamber in the JetCat P90-RXi is 0.4 cm and would have to be increased to 1.6 cm. This increase is simply to maintain the same durability and safety of the old JetCat engines.

IV. Conclusion

The increased demand for small gas turbine engines has led to the need for analysis on how to improve and optimize their performance, so much so that the Air Force put on a competition to support advances in small engine technology. The analysis of JetCat gas turbine engines emphasized the need for improved development on gas turbine engines to support more demanding missions. The results of the real cycle analysis demonstrated that for such an engine to work to the standards given by the Air Force, a compressor pressure ratio of at least 15 would be required. This is a dramatic increase from the pressure ratio of JetCat engines and demands vast improvements to achieve the required performance. Small gas turbine engines primarily utilize centrifugal compressors; however, the requirement for such an increase in pressure ratio demands use of an axial compressor, as that seen in many larger commercial engines. However, such a design change could potentially require modifications to the turbine to support a higher power extraction to drive the compressor and all of its stages. Additionally, the dramatic increase in pressure ratio required greatly increases the turbine entry temperature, leading to the need for blade cooling systems to prevent the blades from deforming and damaging the engine. Depending on the configuration of the engine, the increased pressure ratio can also constrain the combustor design, resulting in added material and therefore weight. The analysis demonstrates the great challenges with small gas turbine engines. Improvements in performance of such engines would require great cost and added complexity in order to sustain performance of the engine with such an increased pressure ratio. Although this is feasible, limitations of materials, limited configurations for rotating parts, and the difficulties associated with small part manufacturing outline just a few of the challenges presented with achieving such a feat.

Appendix A: Code

```
clear all;
close all;
clc;
%% Real Cycle Analysis
% (SLS, T0, TC, CR)
% M0 = [0 .25 0.785 .785];
% T0 = [288.15 288.15 216.65 216.65];
% Tt4 = [1900 1900 1800 1450];

gamma = 1.4;
gamma_t = 1.33;
T0 = 288.15;
R = 287;
a = sqrt(gamma*R*T0);
v = 0;

M0 = v/a;
% Tt4 = 1325.5;
```

```

Tt4 = [1300 1325.5 1400 1600 1800 2000 2200 2400];
% Tt4 = 1325;
% Tt4 = 1325.5;

pi_d = 0.98;
pi_b = 0.98;
pi_n = 0.99;

% pi_c = [2.6 4];
% pi_c = [2 4 8 10 20 26 28 30];
pi_c = linspace(2,35,1000);

cpc = 1005;
cpt = 1157;
% R = 287;

% kerosene, wood fuel, dry peat/coall, parafin wax, butane, propane,
% ethane, methane, hydrogen

% hpr = [44e6, 20e6, 15e6, 45e6, 47e6, 49e6, 50e6, 53e6, 140e6];
% hpr = [15e6, 20e6, 44e6, 45e6, 47e6, 49e6, 50e6, 53e6, 140e6];
hpr = 44e6;

% ec = 0.92;
% ef = 0.92;
% et = 0.92;
% ec = .53;
ec = .92;
ef = 1;
et = .92;
% ec = 1;
% ef = 1;
% et = 1;

% eta_m = 0.99;
% eta_b = 0.99;
% eta_t = 0.92;
% eta_c = 0.42;

% eta_m = 1;
% eta_b = 1;
% eta_t = 1;
% eta_c = 1;

eta_r = 1;
eta_m = .99;
eta_b = .99;
eta_t = .9;
eta_c = .9;

% color = ['r','b','k','g','m','c','y','.'];
tau_lam = zeros(length(Tt4));
a0 = sqrt(gamma.*R.*T0);
for i = 1:length(Tt4)
tau_r = 1+((gamma-1)/2).*M0.^2;
pi_r = tau_r.^((gamma)/(gamma-1));
tau_lam(i) = cpt.*Tt4(i)./(cpc.*T0);
tau_c(i,:) = pi_c.^((gamma-1)/(ec*gamma));

f(i,:) = (tau_lam(i)-tau_r.*tau_c(i,:))./((eta_b.*hpr./(cpc.*T0))-tau_lam(i));
tau_t(i,:) = 1-(tau_r./tau_lam(i)).*((tau_c(i,:)-1)./(eta_m.*(1+f(i,:))));
pi_t(i,:) = tau_t(i,:).^((gamma_t)./(et*(gamma_t-1)));

p0_p9 = 1;
pt9_p9(i,:) = pi_r.*pi_d.*pi_c.*pi_b.*pi_t(i,:).*pi_n*p0_p9;

```

```

M9(i,:) = ((2/(gamma_t-1)).*(pt9_p9(i,:).^((gamma_t-1)/gamma_t)-1)).^(1/2);

T9_T0(i,:) = (cpc/cpt).*tau_lam(i).*tau_t(i,:)./((pt9_p9(i,:)).^((gamma_t-1)/gamma_t));
u9_a0(i,:) = M9(i,).*sqrt(T9_T0(i,)).*sqrt(gamma_t/(gamma));

ST(i,:) = (a0).*((1+f(i,)).*u9_a0(i,)-
M0+(1+f(i,)).*(1/gamma).*T9_T0(i,)).*(1./u9_a0(i,)).*(1-p0_p9));
sfc(i,:) = f(i,)./(ST(i,));
sfc_eng(i,:) = 35304.*sfc(i,);
ST_eng(i,:) = 3.28084.*ST(i,);

% eta0 = a0.*M0.*ST.*(1+fb)./(f.*hpr)
eta_th(i,:) = a0.^2.*((1+f(i,)).*u9_a0(i,).^2-M0^2)./(2*f(i,).*hpr);
eta_p(i,:) = 2.*ST(i,)*M0./(a0.*((1+f(i,)).*u9_a0(i,).^2-M0^2));
eta_0(i,:) = eta_th(i,).*eta_p(i,);

hold on
% plot(pi_c,eta_0(i,:),color(i))
plot(pi_c,eta_th(i,:))
xlabel('\pi_c')
ylabel('\eta_th')
legend('1300','1325','1400','1600','1800','2000','2200','2400')
end

figure
for j = 1:length(Tt4)
hold on
plot(pi_c,ST_eng(j,:))
xlabel('\pi_c')
ylabel('ST')
end
id = 1800*ones(length(ST_eng));
plot(pi_c,id)
legend('1300','1325','1400','1600','1800','2000','2200','2400','Requirement')

figure
for k = 1:length(Tt4)
hold on
plot(pi_c,sfc_eng(k,:))
xlabel('\pi_c')
ylabel('TSFC')
legend('1300','1325','1400','1600','1800','2000','2200','2400')
end
ideal = .87*ones(length(sfc));
plot(pi_c,ideal)
legend('1300','1325','1400','1600','1800','2000','2200','2400','Requirement')

figure
mesh(pi_c,sfc,ST)
xlabel('pi_c')
ylabel('sfc')
zlabel('ST')

% T = 24.376e3;
% m_dot = T/ST;
% m_dot_eng = 2.20462*m_dot
%
%
% ML = 406122.63+205800;
% MTO = 767318.226;
% TSFC = 1.6.*sfc;
% L_D = 20.5;

```

```

% g = 9.81;
% RF = a0*M0*L_D/(g*TSFC);
% Range = RF*log(MTO/ML)

%% Nathan Genrich, Crawford Leeds, Tyler Smith
% http://web.mit.edu/16.unified/www/FALL/thermodynamics/notes/node123.html
% Thermal analysis for blade cooling

clc; clear all; close all;

% inputs
Tmelt = 1673; % Melting temp of inconel
Tburner = 2200; % [K] Burner temp
T1 = 288; %K Inner temperature of fluid in blade
T1 = linspace(288,Tburner);
T2 = Tburner; %K effectively the burner temperature
A = 0.005; %m^2 Linearized surface area of blade (jetcat p90 rxi)

h1 = 7; % [W/m^2-K] heat transfer coefficient inside blade
h2 = 7; % heat transfer coefficient outside blade
k = 6.5; %[W/m-K] Thermal conductivity of inconel
L = .002; % [m] hollow thickness of blade

Tw2 = 0; %outer wall temp (max temp) of blade
Tw2 = T2 - (T2 - T1) ./ ( h2./h1 + L.*h2./k + 1);

if Tw2 < Tmelt
    fprintf('Tw2 = %6.2f and the bland will NOT melt\n',Tw2);
else
    fprintf('Tw2 = %6.2f and the bland will melt\n',Tw2);
end

figure
plot(T1,Tw2)
hold on;
plot([T1(1) T1(end)],[Tmelt Tmelt],'r--')
hold on;
plot([T1(1) T1(end)], [Tburner Tburner],'m-')
xlabel('Inner Fluid Temperature (K)')
ylabel('Outer Wall Temperature of Turbine Blade (K)')
legend('Blade Temp vs Inner Fluid Temp','Melting Temp of Inconel','Burner
Temperature')
% axis([0 (T1(end)+50) 0 Tw2])
axis([0 T1(end)+50 800 Tburner+50])

```

Acknowledgments

The team would like to thank Professor Kantha for his knowledge and enthusiasm about all things propulsion. The team would also like to thank Kevin Dimond for providing useful, pertinent feedback on all assignments

References

¹"Military Turbojet/Turbofan Characteristics." N.p., n.d. Web. <<http://www.jet-engine.net/miltfspec.html>>.

²Principles of Propulsion: Extracts from ASEN 4013